



Ceiling temperature assessment of a reduced scale tunnel in the event of two hydrogen jet fires

Shibani^{1,2} · Fatemeh Salehi¹ · N. Suresh Kumar Reddy² · Salman Jalalifar¹ · Rouzbeh Abbassi¹

Received: 7 May 2021 / Revised: 14 July 2021 / Accepted: 22 July 2021 / Published online: 5 August 2021
© The Author(s), under exclusive licence to Springer Nature Switzerland AG 2021

Abstract

It is critical to comprehend the safety aspects of hydrogen fuel cell vehicles (FCVs) in semi-confined and confined environments. The hydrogen jet fire is a key hazard resulting from coincidental hydrogen release from onboard storage followed by ignition. The rise in temperature and depletion of oxygen inside the tunnel may cause calamitous debacles. In this study, comprehensive computational fluid dynamics (CFD) simulations were designed to understand the interactions of multiple hydrogen fires in a confined environment. CFD simulations for hydrogen and liquefied petroleum gas (LPG) jet fires were conducted inside a reduced scale model tunnel. The model is initially validated against the experimental data for a single LPG fire scenario. A parametric study was then made to understand the impact of the fire location in the tunnel and the ventilation velocity. The results show an increasing-decreasing trend in the temperature over the two fire sources before the temperature reaches a quasi-steady state for the cases without ventilation speed. However, in the presence of ventilation velocity, the temperature rises are seen until a quasi-steady-state is reached. The vicinity of the two flames in the tunnel influences ignition proficiency, dependent on the heat feedback enhancement and air supply restriction instruments. A temperature drop was seen at the ceiling as we move along the passage length. The ventilation velocity influences the proportion of fuel and oxygen, driving the burning proficiency to either increase or decrease. The overall ceiling temperatures were seen to reduce in the presence of higher ventilation velocity. In conclusion, for hydrogen and LPG fire interaction, a distinction in the ceiling temperature pattern was seen between the two because of the disparity in the emissivity of the two fuels.

Keywords Computational fluid dynamics (CFD) · Multiple hydrogen jet fires · Tunnel fire · Safety assessment

Introduction

Non-renewable fuels such as natural gas, oil, and coal, which cannot meet the worldwide energy utilization, will ultimately consume. On the other hand, the rising concerns about environmental pollution and greenhouse gas emissions brought about by fossil fuels prompt us to develop cleaner and environmentally friendly power resources. Among different clean energy assets, there is an extraordinary interest in hydrogen because of its pollution-free qualities (The Future of Hydrogen 2019). Hydrogen shows a high-energy yield,

natural advantages as well as industrial competitiveness (Staffell et al. 2019). The world is now experimenting with hydrogen energy in all spaces, especially in the transport sector, such as fuel cell vehicles (FCVs) (Manoharan et al. 2019). However, FCVs' safety aspects, particularly in semi-confined and confined environments such as tunnels, require detailed analysis under various circumstances (Abohamzeh et al. 2021). Hydrogen is not detectable by human senses due to its colourless, odourless, tasteless, and non-poisonous nature (Lewis and von Elbe 1987). While natural gas and propane are also odourless, sulphur-containing odorants are added to them to make them detectable (Berman 1986). In the case of hydrogen, no such odorant is available to match hydrogen's dispersion rate. Hydrogen is 14 times lighter than air and 57 times lighter than gasoline (Babrauskas 2003). If it releases outside in an open space, it will rise and disperse rapidly. However, in confined spaces, accumulation can cause a hazard due to its broad flammable limit in the air varying from 4% to 75% (Hord 1976). Due to hydrogen's small molecule and low

✉ Fatemeh Salehi
fatemeh.salehi@mq.edu.au

¹ School of Engineering, Macquarie University, Sydney, Australia

² Mechanical Engineering Department, Birla Institute of Technology & Science Pilani, Hyderabad, India

viscosity, it is prone to leakage (McCarty et al. 1981; Rigas and Sklavounos 2005).

A few experiments have been conducted to study the aspect of tunnel fire (Gu et al. 2020; Wu 2008; Hao et al. 2020; Król et al. 2019; Huang et al. 2018; Gannouni and Maad 2017; Li 2019), however, they are limited due to the exorbitant costs and security contemplations for the trial tests. Computational fluid dynamics (CFD) simulation methods have tackled the above concern (Hwang and Edwards 2005) as they are cost-effective, allowing for comprehensive analysis. Gu et al. (2020) used CFD simulations to reproduce hydrogen jet fire for transport vehicles inside a 102 m tunnel based on Wu (2008), focusing on various elements including hydrogen leakage rate, jet fire area, jet fire location, and ventilation. The results showed that with an addition in hydrogen release rate, ceiling temperature and hydrogen dispersion rate increase; however, a rise in the release rate could control the dispersion interaction. On the other hand, longitudinal ventilation can reduce the tunnel's overall temperature yet may bring down the high-temperature layer. Wu (2008) had created a full-scale CFD model of hydrogen jet fire in a 5 m × 5 m cross-sectional area tunnel with a length of 102 m. The effect of ventilation velocity on downstream flame and upstream backlayering phenomenon was studied. The results showed that the hydrogen release rate plays a crucial role in determining the effect of ventilation velocity. For lower hydrogen release rates, the ventilation velocity does control the downstream flame and eliminates the upstream backlayering. However, for more significant hydrogen release rates, a hydrogen layer deficit of oxygen was seen along with the downstream due to the insufficiency in airflow. This could pose a secondary hazard in the tunnel. Hao et al. (2020) studied the hydrogen leakage and emission of FCVs in confined spaces to analyse their safety standards. An appropriate test method was designed for a seal chamber test to evaluate the safety of the vehicle. The results showed a 0.0004% hydrogen concentration near the vehicle for the hydrogen leakage test, whereas a value of more than 2300 ppm of hydrogen concentration for the emission test. Based on this, safety standards for hydrogen FCVs were proposed for confined spaces. Other experiments based on tunnel fires have also been conducted apart from hydrogen fires (Król et al. 2019; Huang et al. 2018; Gannouni and Maad 2017). The investigation of Król et al. (2019) on air velocity distribution in a tunnel is another example. It was found that the difference between modelled and measured data was less than a 9% deviation; however, the deviations were more considerable, close to the walls of the tunnel. Huang et al. (2018) conducted CFD simulations for modelling jet fire with different heat release rates and sealing ratios. It was seen that roof temperature ascends with the sealing ratio, taken as the fraction of sealing height over the entrance height. Gannouni and Maad (2017) studied the effects of longitudinal ventilation

in the case of a tunnel fire. The ventilation and fire's inertia and buoyancy forces affect the backlayering spread. An increase in the backlayering arrival time was observed as the ventilation velocity was increased, but a decrease was observed for an increase in the heat release rate. Li (2019) further studied fire and explosion for various fuel vehicles in tunnels. Pool fires, jet fires and fireball hazards were studied for liquid fuels, liquefied fuels, compressed gases, and batteries. In the case of pool fire, it was observed that liquid fuels pose equivalent hazards compared to traditional fuels, but liquefied fuels are more dangerous and pose a greater risk. Fires were more prominent in size for pressurized tanks but had a shorter duration. The jet fires from the gas release were seen to be transient. Whereas in the case of hydrogen vehicles, the fire sizes are significantly large compared to CNG tanks. The explosion due to tank rupture could be tolerated from a distance of 100 m, but in the case of cloud explosion, the scenario was extremely severe and intolerable for tunnel users (Li 2019).

Despite previous studies on the single jet fire, there is a lack of understanding of the hydrogen jet fires, especially for multiple jet fires that may bring about more disastrous conditions, such as fire blending and shifting change the fire height (Liu et al. 2013). This study focuses on demonstrating how two hydrogen jet fires' interact inside a tunnel. The simulations were conducted for two hydrogen jet fires inside a reduced-scale tunnel (Hu et al. 2013). A comprehensive study was performed to understand the impact of the distance between the jet fires, the distance of the first fire source from the tunnel entrance and the ventilation velocity. This study will assist the assessment of the hydrogen jet fires inside a tunnel consequences, providing guidelines for evaluation, restricting the danger and keeping an essential distance from an auxiliary disaster.

Methodology

Governing equations

Fire dynamics simulator (FDS) software is used to conduct the simulations. FDS is an open-source code that has been widely employed for fire simulations. A large eddy simulation (LES) framework is adopted to numerically solve the Favre filtered equations for the conservation of mass, momentum, species mass fraction, and energy for low Mach number applications (Gu et al. 2020). The transport equations for the conservation of mass, momentum, and kinetic energy are expressed as

$$\frac{\partial \bar{\rho}}{\partial t} + \frac{\partial \bar{\rho} \tilde{u}_i}{\partial x_i} = 0 \quad (1)$$

$$\frac{\partial \overline{\rho u_i}}{\partial t} + \frac{\partial \overline{\rho u_i u_j}}{\partial x_j} + \frac{\partial \overline{p}}{\partial x_i} - \frac{\partial \overline{\sigma_{ij}}}{\partial x_j} = -\frac{\partial \overline{\rho \tau_{ij}^r}}{\partial x_j} + \frac{\partial}{\partial x_j} \left(\overline{\sigma_{ij}} - \overline{\sigma_{ij}} \right) \quad (2)$$

$$\frac{\partial E_f}{\partial t} + \overline{u_j} \frac{\partial E_f}{\partial x_j} + \frac{1}{\rho} \frac{\partial \overline{u_i p}}{\partial x_i} + \frac{\partial \overline{u_i \tau_{ij}^r}}{\partial x_j} - 2\nu \frac{\partial \overline{u_i S_{ij}}}{\partial x_j} = -\epsilon_f - \pi \quad (3)$$

where ρ is the density, p is the pressure, u is the velocity, and T is the temperature. τ_{ij}^r shows the resolved stress tensor whereas σ_{ij} expresses the shear stress tensor. E_f is the kinetic energy, ν is the Poisson's ratio, S_{ij} is the strain tensor, ϵ_f is the dissipation of resolved kinetic energy, and π is the sub-filtered scale of dissipation of kinetic energy. Overbars and tildes denote Reynolds and Favre filters, respectively. To close the governing equations, models for subgrid turbulence and combustion are required. Here we adopted the Smagorinsky model for the subgrid-scale turbulent viscosity and a combustion model based on the mixture fraction concept with infinitely fast chemistry is considered. (McGrattan et al. 2017).

Test cases studied

The main aim of the current study is to analyse multiple hydrogen fire interactions. For this purpose, we considered a reduced scale model of a tunnel, which is similar to the experiment of Hu et al. (2013). The tunnel had dimensions of 6 m (length) \times 1.3 m (width) \times 0.8 m (height), with its ceiling and side walls made of concrete. The ambient temperature, pressure, oxygen mass fraction, and relative humidity inside the tunnel were taken as 20.0 °C, 101325 Pa, 0.23 kg/kg, and 40.0%, respectively (Hu et al. 2013). The material properties of concrete, including density, specific heat, conductivity and emissivity, were considered 2280.0 kg/m³, 1.04 kJ/(kg·K), 1.8 W/(m·K) and 0.9, respectively.

The schematic view of the case is shown in Fig. 1 while a list of parameters for simulation cases is given in Table 1. Case 0–1 and Case 0–2 were conducted for single hydrogen fire, while Cases 1 to 7 included multiple hydrogen fires to analyze the effects of the distance between the fires, the distance of the first fire source from the entrance, and the ventilation velocity (i.e. the inlet longitudinal airflow speed). To compare hydrogen jet fires with hydrocarbon fuel fires (Salehi et al. 2015), two liquefied petroleum gas (LPG) cases are also considered. The first LPG case (Case 8) is considered to validate the CFD model against the experimental data (Hu et al. 2013), while the second LPG case (Case 9) is considered to compare multiple LPG fires with multiple hydrogen jet fires (Case 1).

The burners have dimensions of 0.3 m \times 0.3 m \times 0.03 m (Hu et al. 2013) in all cases. A fixed heat release rate (HRR) for both fuels was selected based on the previous studies. In hydrogen cases, the fire sources have an HRR of 801 kW, while for the LPG cases, it is 120 kW. The heat release rate

Table 1 A list of parameters for simulation cases

Case	Fuel	Distance between the first fire source and the tunnel's entrance (m)	Distance between the jet fires (m)	Ventilation Velocity (m/s)	Heat release rate (kW)
0–1	H ₂	0.775	0	0	801
0–2	H ₂	2.325	0	0	801
1	H ₂	0.775	1.55	0	801
2	H ₂	0.775	3.1	0	801
3	H ₂	1.55	1.55	0	801
4	H ₂	0.775	1.55	0.5	801
5	H ₂	0.775	1.55	1	801
6	H ₂	0.775	1.55	1.5	801
7	H ₂	0.775	1.55	2	801
8	LPG	0.775	1.55	0	120
9	LPG	0.775	0	0	120

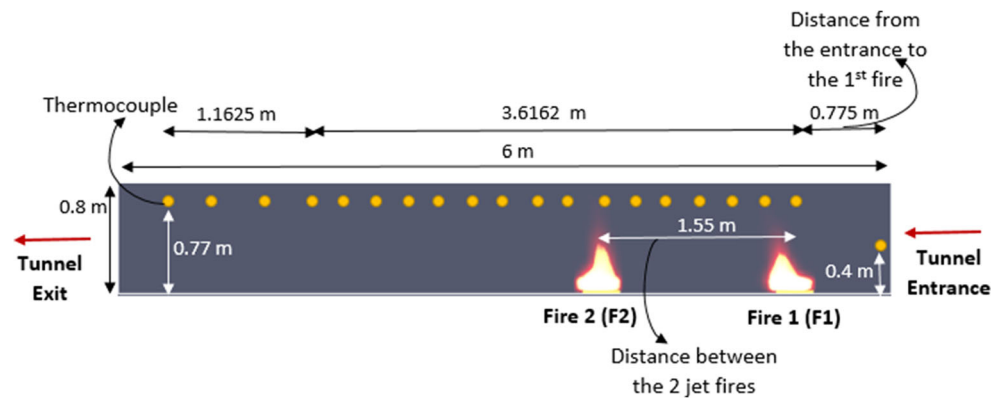
per unit area (HRRPUA) was computed using the HRR values and the fire surface area, which was taken as 0.09 m². The specific heat of combustion for hydrogen and LPG are 141.80 MJ/kg and 51 MJ/kg, respectively (Gu et al. 2020; Hu et al. 2013). A simple chemistry approach was adopted for both fuels. It assumes that the reaction of the fuel and oxygen is fast and controlled only by mixing. All fire source surfaces except the top surface were set as inert. The exit of the tunnel is taken as an open surface that applies zero pressure field. For the cases with zero inlet velocities, the entrance is also set as an open surface while for the cases with non-zero inlet velocities; it was set as an inlet with a constant air velocity. The floor surface was set as inert.

As shown in Fig. 1, nineteen thermocouples (monitoring points) were considered at the height of 0.77 m from the ground along the central ceiling line of the tunnel to measure the ceiling temperature. Out of which, 15 of them were placed from 0.775 m onwards from the entrance with a separation distance of 0.2583 m. The last four were placed with a separation distance of 0.3875 m. One thermocouple was placed at the entrance at the height of 0.4 m from the ground level to measure the entrance temperature. The total simulation time for each case was taken to be 100 s, which is long enough to ensure a quasi steady-state condition was achieved. This is selected based on the realistic hydrogen release conditions (Wu 2008) where, for example, a 6 MW hydrogen fire lasted for about 60s.

Mesh study

A mesh study was conducted for a single jet fire with zero ventilation velocity (Case 0–1). The first, second and third meshes have a homogenous mesh distribution with a cell size

Fig. 1 Schematic view of the simulation set up for multiple jet fires (Case 1)



of $0.2 \times 0.2 \times 0.2$ m, $0.1 \times 0.1 \times 0.1$ m and $0.05 \times 0.05 \times 0.05$ m. For the fourth and fifth meshes, the grid was refined near the ceiling and jet fire regions (Huo et al. 2015) with a cell size of $0.025 \times 0.025 \times 0.025$ m and $0.0125 \times 0.0125 \times 0.0125$ m respectively, as shown in Fig. 2.

The recommended mesh sizes range from 1/5 to 1/20 of D^* , where D^* is a characteristics fire diameter based on the heat release rate of the fire and the ambient thermal condition (Wang et al. 2016). This ensures at least a moderate level of accuracy in modelling the plume (McGrattan et al. 2017; Wang et al. 2016). Figure 3 shows the statistically steady-state ceiling temperature above the fire source. It can be seen that the temperature is initially sensitive to the mesh size, while with further refinement; the temperature is marginally changed, confirming the third mesh was suitable for jet fire simulations.

Case validation

To validate the model, the simulation results are compared with the published experimental data, which were obtained by Hu et al. (2013) for the LPG case with 120 kW heat release rate and 1.2 m/s ventilation velocity (Case 9). The temperature along the ceiling is important since it affects the reliability of the structure in tunnels. Hence, the dimensionless temperature is computed using $\frac{T - T_\infty}{T_{Ref} - T_\infty}$, where T_{Ref} is the maximum ceiling temperature for a case, T is the temperature at location X on the ceiling and T_∞ is the ambient temperature (Hu et al. 2013). The results are presented in Fig. 4 after the quasi-steady state condition was achieved. It shows the dimensionless

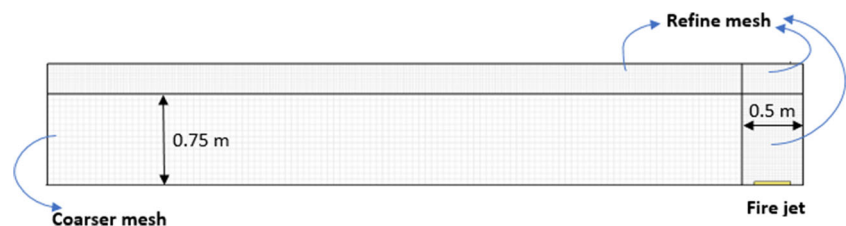
temperature along with the tunnel length from the fire source, $\Delta X = X - X_f$, where X is the distance from the entrance and X_f is the location of the fire source measured from the entrance. In the case of multiple jet fires, X_f is the location of the first fire source from the entrance. As can be seen, the agreement between the simulation and measurements is satisfactory, confirming the accuracy of the model.

Results and discussion

Effect of the location of fire sources

In this study, the direction of the jet fire flames is vertical (perpendicular to the ground). Vertical flames are considered in many studies focusing on their effects on the ceiling structure (Hu et al. 2013; He et al. 2019; He et al. 2021; Wang et al. 2020; Zhang et al. 2020). The impact of vertical flames is different if the flame jet is horizontal. Due to the gravity effect, in the case of vertical flames, better mixing of fuel and air occurs that enhances the combustion process. However, horizontal jet fire flames are wider and have a greater flame area compared to vertical flames, because the gravity pushes down the released fuel. Vertical jets pose a high risk for objects placed near the exit orifice, whereas horizontal jets are in general more hazardous due to flame impingement and high emissive power (Palacios and Rengel 2020). Horizontal flames are not in the scope of this study but they will be conducted in our future studies.

Fig. 2 Schematic mesh design for the single fire source in the tunnel



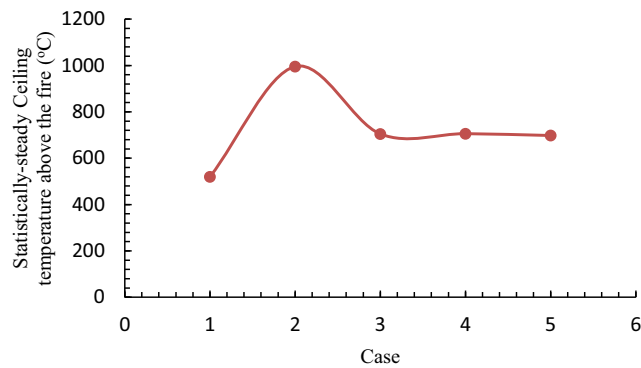


Fig. 3 Mesh independence study

To provide an overview of the effect of different parameters, the counterplots of temperature at 100 s of physical time are shown in Fig. 5 for all hydrogen cases. Fires with significant heat release rates in confined regions such as tunnels are obstructed by the tunnel ceiling, causing the flame to split and spread on the ceiling, as presented in Fig. 5 for all the cases. It can be observed that the buoyancy affects the flame in a restricted zone, which is consistent with the previous observation in the study of Zhao and Fan (2020). The location of the jet fires plays an important role in either enhancing the combustion process or diminishing it. Cases 1, 2 and 3 were compared to comprehend the dependency of combustion efficiency on factors such as the distance between the two fires and the closeness to the tunnel entrance. Heat feedback enhancement and air supply restriction are two mechanisms that influence the burning pattern of the multiple fires based on the location of the fire flames (Manoharan et al. 2019). The heat from one flame enhances the combustion efficiency of the other flames in the vicinity of radiation, while in the case of smaller fire spacing, the air supply to the inner fires may be restricted, which subsequently decreases the combustion efficiency. The decrease in combustion impacts the heat enhancement and hence ultimately diminishes the combustion efficiency of the multiple fire-burning scenarios. However, the increase in the spacing between the fires decreases the effect

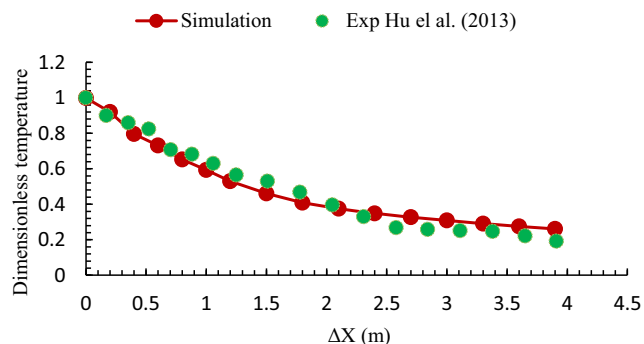


Fig. 4 Comparison of the LPG single jet simulation with the experimental data

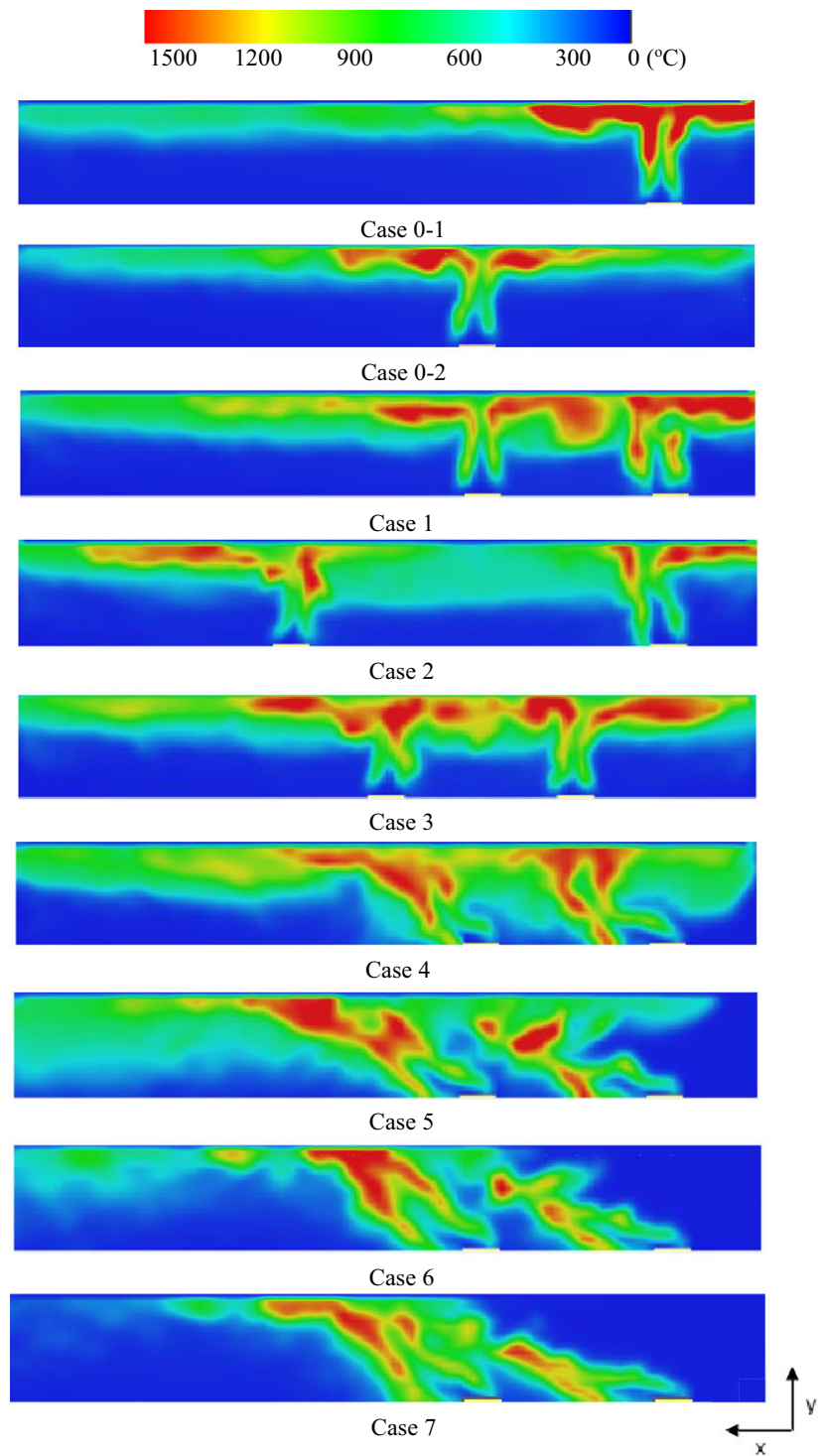
of the heat enhancement mechanism prompting the decline of the burning rate. Nevertheless, the combustion should improve as the spacing is increased due to the increase in the available air supply from ambient surroundings. The abundance of air supply affects the air pressure gradient in the combustion zone, resulting in vertically weak flames causing a decreased heat feedback. This competition between the two mechanisms leads to complex variations, as discussed further in the following (Manoharan et al. 2019).

The ceiling temperature above the jet fires for Cases 0–1, 0–2, 1 and 2 are presented in Fig. 6, showing an increasing and then decreasing trend before reaching a statistically steady-state condition after approximately 68 s. F1 (solid lines) and F2 (dashed lines) refer to the ceiling temperature above the first and second fires in the cases with multiple fire sources, respectively. For single jet fire cases (Cases 0–1 and 0–2), as the fire position moves further away from the entrance, the quasi-steady-state ceiling temperature declines from 835 °C to 490 °C. While the jet fire is away from either the entrance or the exit, the air supply to the fire is inhibited and hence we see such a trend. Comparing Case 0–2 and Case 1 shows that the quasi-steady-state ceiling temperature for Case 0–2 was even less than Case 1 (both F1 and F2) because of the absence of another fire, the effects of the heat feedback mechanism vanish (for Case 0). However, the ceiling temperature above the second fire (F2) in Case 1 is lower than that of F2 in Case 2 due to the insufficiency of the air supply near Case 1, which is a prerequisite for combustion. The ceiling temperatures above the first fire in Cases 1 and 2 show similar trends with minor deviations.

The quasi-steady-state ceiling temperature along the tunnel is illustrated in Fig. 7 for Case 0, 1 and 2. As noted previously, $\Delta X = 0$ refers to the location of the first fire, which is closer to the entrance. It can be seen that in single jet scenarios (Case 0), the ceiling temperature decreases from the location above the fire source as we move along the tunnel towards the exit, which is consistent with the previous study (Hu et al. 2013). It should be noted that the temperature is plotted versus the relative distance from the fire source, and hence for Case 0–2, it ends at 3.6 m. The trend is completely different in multiple jets cases since a significant depletion was noticed in the ceiling temperature between two fires. This increases as the distance between two jet fires increases; keeping the first fire position constant (Cases 1 and 2). This is due to the reduction in fire interactions, i.e. inhibition in fire merging near the ceiling, which accounts for the temperature between the fires.

Figures 8 and 9 compare Case 1 and 3 to understand the effect of the first fire source location from the entrance. The plot for the temperature above both fire sources (Case 3) is similar to that of the single jet fire (Case 0–1) due to its proximity to both the exit and the first jet fire where the air is

Fig. 5 Temperature variation 2D slice view along the enclosure centre-line at 100 s (tunnel entrance to exit is from right to left of the slice view)



available to direct the combustion process. The temperature is also affected by the heat feedback mechanism due to the presence of a secondary source. Particularly, the combustion efficiency depends upon the jet fire location. Figures 8 and 9 demonstrate that moving from the entrance does initially reduce the combustion efficiency while moving farther away

increases the combustion efficiency due to the availability of air closer to the tunnel exit.

Finally, we monitored the temperature at the entrance for all the hydrogen cases, as shown in Fig. 10. It was observed that the burning rate affects the entrance temperature. For Case 0, as expected, the entrance temperature decreases as the

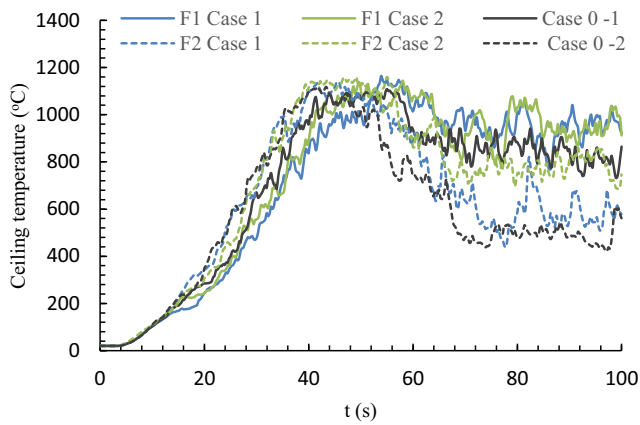


Fig. 6 Temporal evolution of the ceiling temperature above the fire source

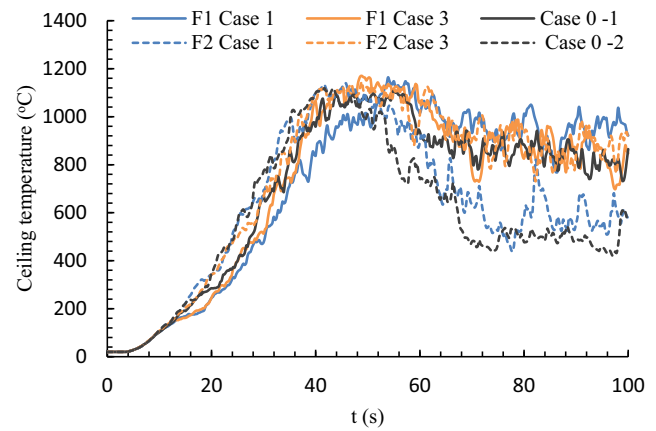


Fig. 8 Ceiling temperature above fire vs time

distance between the fire source and the entrance increases (0–2 compared to 0–1). For multiple jet fire cases (Cases 1–3), the temperature rise is faster than the single jet due to the jet fire interactions. However, the effect of the distance between the fire source and the location of the first fire source is marginal on the entrance temperature.

Due to the scarcity of studies on multiple hydrogen jet fires, LPG cases were also considered for comparison. For the given fire spacing, the two mechanisms (heat feedback enhancement and air supply restriction) may influence the interactions of the flames in a competitive manner to justify the above results, which is also in line with the experiment conducted by He et al. (2019) to understand the behaviour of multiple fires of heptane. Flame merging was observed in He et al. (2019), however, this does not occur in the cases considered in this study, as the fires were not close enough. Besides, in the absence of ventilation velocity, the tilting of flames towards each other was not observed in our cases due to the spreading of the fire flame crown at the ceiling of the tunnel, which caused the jet fire flames to touch each other at the ceiling (He et al. 2019; He et al. 2021). Fire touching, tilting and merging occur due to the pressure difference caused by

airflow restriction to the inner fires (He et al. 2019). With smaller fire spacings as shown for Case 1 and 3, the flames were seen to touch near the ceiling owing to a higher temperature profile compared to Case 2. The temperature profiles for the cases considered in this study showed an exponential decay when moving away from the fire sources. This is consistent with the observations made by Wang et al. (2020) for propane fuel.

Effect of ventilation velocity

The wind can both feed the fire and put it off. A fire can be sustained only by having a proper ratio of fuel and oxygen within certain limits. At low wind speeds, only the combustion products are replaced by oxygen, which in return combines with the vaporized fuel. The process is faster due to the availability of more oxygen, leading to an increase in heat density that enhances combustion (Finney and McAllister 2011). However, with sufficiently higher wind speeds, the fire can be blown off. At high wind speeds, the vaporised fuel and combustion products are removed before they mix with the oxygen, thus lowering the heat density and ultimately blowing off the fire (Zhao and Fan 2020). Since the hot combustion

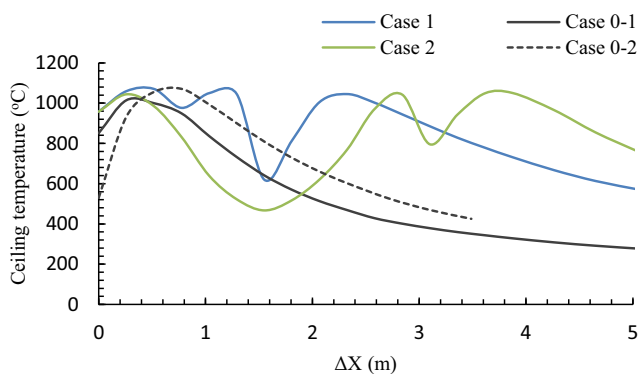


Fig. 7 Statistically steady-state ceiling temperature distribution along the tunnel length

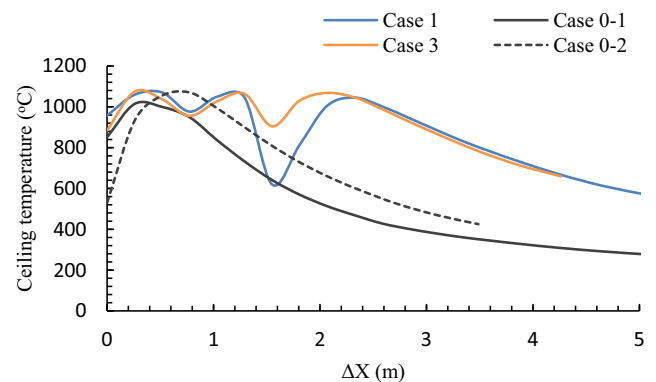


Fig. 9 Statistically steady-state ceiling temperature distribution along the tunnel length

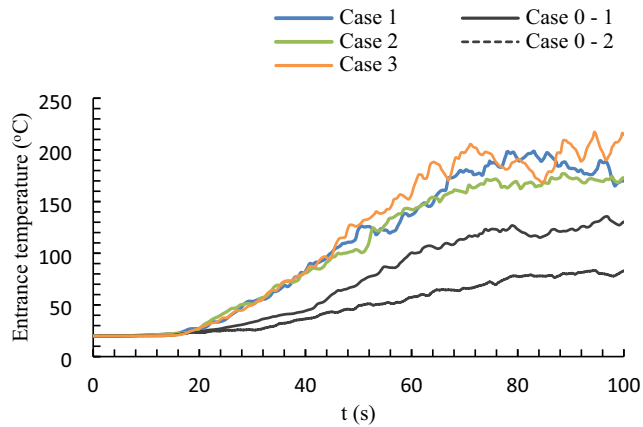


Fig. 10 Entrance temperature over time

products and the vaporised fuel are removed, the overall temperature inside the tunnel reduces gradually, aiding in controlling the hazard.

Figures 11 and 12 show the temporal and spatial variation of ceiling temperature, respectively, for Cases 1, 4–7. In the presence of ventilation velocity (Case 4–7), the ceiling temperature increased and then reached a statistically steady-state value, which is different from Case 1 where the ventilation velocity was taken as zero (Fig. 11). Due to the lower density of hydrogen compared to air, the flames were vertically spread inside the tunnel in the absence of ventilation velocity i.e. Case 1. In the presence of ventilation velocity, the flames were seen to be tilted (Cases 4–7) as shown in Fig. 5. The ventilation velocity suppressed the high gas temperature layer upstream of the tunnel (Fig. 5), which was more prevalent in the cases with higher ventilation speeds (Cases 6 & 7). On the other hand, the downstream faced higher temperatures as the light hot gas layer was displaced towards the end of the tunnel (Cases 4–7). A thinner hot gas temperature layer near the downstream ceiling was observed with a further increasing the ventilation velocity (Cases 6 & 7 compared to Cases 4 & 5), thus reducing the ceiling temperatures even more by taking

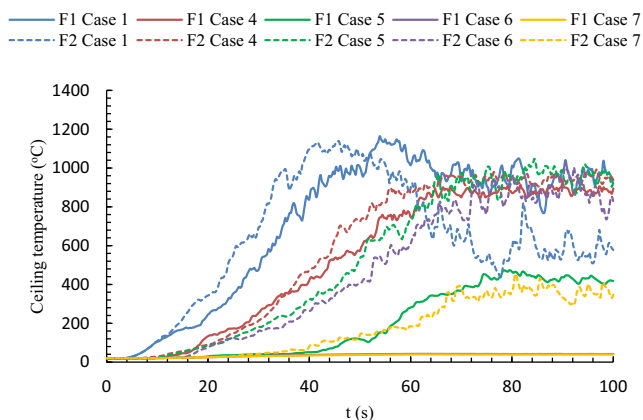


Fig. 11 Ceiling temperature above fire versus time

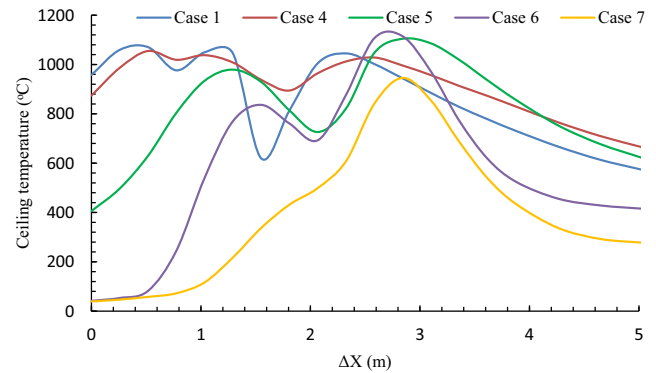


Fig. 12 Statistically steady-state ceiling temperature distribution along the tunnel length

the generated heat away (Case 7). Both jet fire flames were seen to tilt away from the entrance due to the ventilation velocity where the first fire flame bent towards the second. The angle of tilt of the flame increased with an increase in ventilation velocity (Cases 4–7). These observations were consistent with the study of Gu et al. (2020) for the hydrogen fuel and the study of Zhang et al. (2020) for the propane fuel.

The ceiling temperature above the first fire's location (F1) was far more affected compared to that at the second fire's location (F2) for higher ventilation velocities. As the ventilation velocity increased, the ceiling temperature above the fire sources (F1 & F2) decreased. The ceiling temperature was noted as 20 °C above the first fire (F1) in Cases 6 and 7 (also having coinciding plots), which remained constant throughout the time, due to the titling of the flames. The presence of ventilation velocity affected the flame splitting at the ceiling as shown in Fig. 5. With zero ventilation velocity (Case 1), the temperature drop at the jet fire location was observed while for Cases 4–7, it did not occur. The ceiling temperature above the second fire (F2) for Cases 4–6 were higher compared to that in Case 1 due to the tilting and touching of the first and second fire flames. The obtained results are consistent with the study of Zhang et al. (2020) that also focused on the impact of ventilation velocity on multiple jet fires. Further increasing the ventilation velocity resulted in an overall decrease in the ceiling temperature due to both tilting and the cooling effect as the hot gases were transferred out (Case 7). The impact of ventilation velocity is clearly shown in the quasi-steady-state ceiling temperature profiles (Fig. 12). The temperature towards the end of the tunnel decreases in the sequences Case 4, Case 5, Case 1, Case 6, and Case 7.

Hydrogen and LPG jet fires

The hydrogen and LPG jet fires interact differently due to the difference in their burning nature. The specific heat of combustion and ignition temperature for hydrogen are 141.80 MJ/kg

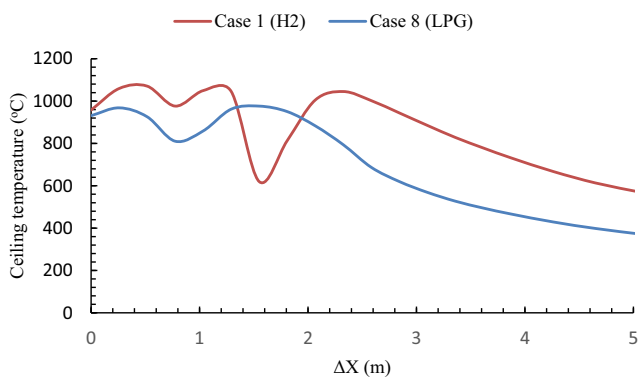


Fig. 13 Statistically steady-state ceiling temperature distribution along the tunnel length

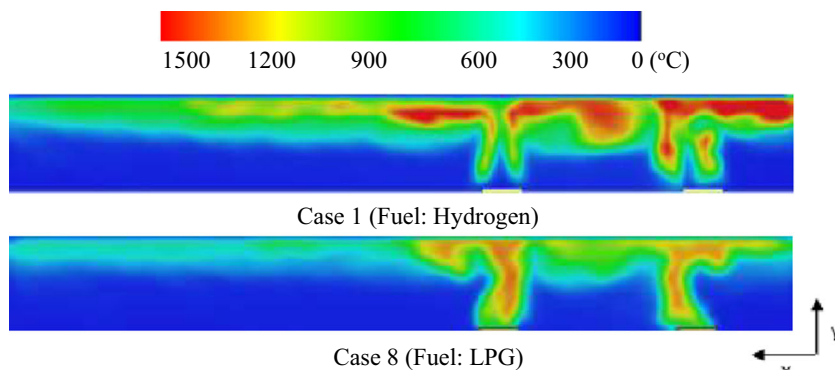
and 585° C, respectively, whereas for LPG they are 51 MJ/kg and 470 °C, respectively. The HRR for hydrogen and LPG were taken to be 801 kW and 120 kW as noted in Table 1. The emissivity of a flame influences the total flux of heat radiated. Compared to hydrocarbons (in our case LPG), the low emissivity of hydrogen flame shows a lower heat transferred by radiation to objects near the flame or a secondary flame (NREL U.S. 2009). Hydrocarbon-based fuel flames radiate more heat than hydrogen flames, and hence the heat transfer from one flame to another flame increases that enhance the combustion efficiency. On the other hand, the heat release rate of LPG was significantly less compared to the hydrogen case, justifying why the overall ceiling temperatures for LPG flames were lower than that of hydrogen flames. As shown in Fig. 13, for the hydrogen case (Case 1) the ceiling temperature above the second hydrogen fire (F2) is lower than F1. In contrast, the opposite trend is observed in the LPG case (Case 8). This happened because the heat feedback efficiency for LPG is higher than hydrogen, which aids the combustion process. Figure 14 shows temperature variation 2D slice view along the enclosure centreline at 100 s. It can be comprehended that the flame splits in case of hydrogen jet fires which does not happen for LPG case, due to the higher HRR of hydrogen compared to LPG, in a reduced scale model. Due to the splitting of

flame, a ceiling temperature drop was observed just above the hydrogen jet fire source, although this does not occur in the LPG fire case as observed in Fig. 14.

Conclusion

Large eddy simulations of multiple vertical hydrogen fires in a scaled tunnel were conducted. The spatial ceiling temperature along the tunnel length, the entrance temperature and temporal development of the ceiling temperature were determined to contemplate the impact of the jet fire positions. It was seen that the ceiling temperatures were influenced by the positions of the two fires and the ventilation velocity. It was found that heat feedback enhancement and air supply restriction simultaneously affect the burning rate. The vicinity to the tunnel’s entrance and/or tunnel’s exit affects the air supply accessibility, which drives the burning cycle. Further, the closeness of the flames builds up heat feedback, which improves the ignition effectiveness. In the presence of high ventilation velocity, the ceiling temperatures decreased. The ventilation velocity feeds the fire in its lower ranges and put it off when increased further. Tilting of fire flames was also observed in the cases with high ventilation velocity. The entrance temperature was marginally affected for the cases where the ventilation velocity was zero, although it reached the ambient temperature as the ventilation velocity was increased. Finally, the hydrogen multiple jet fires scenario was compared with a hydrocarbon fuel case i.e. liquefied petroleum gas (LPG) multiple fires scenario. Significant differences in the ceiling temperature trend were observed between the two cases due to the difference in the emissivity of the fuels. Having a higher emissivity, LPG enhances the heat feedback efficiency, due to which the combustion of the second propane jet fire from the entrance was aided efficiently. Therefore, an in-depth study is required to understand hazardous scenarios better.

Fig. 14 Temperature variation 2D slice view along the enclosure centre-line at 100 s (tunnel entrance to exit is from right to left of the slice view)



Nomenclature T [°C], Temperature; x [m], Distance; i [-], Cartesian axis direction; j [-], Cartesian axis direction; t [s], Time; $\bar{\rho}$ [kg/m³], Filtered density; \bar{p} [N/m²], Filtered pressure field; τ_{ij}^r [N/m²], Sub-grid stress tensor for the Favre-filtered momentum; $\tilde{\sigma}_{ij}$ [N/m²], Shear stress tensor; E_f [J], Kinetic energy of the filtered velocity; ν [-], Poisson's ratio; \bar{S}_{ij} [1/T], Filtered rate-of-strain tensor; ϵ_f [J/s], Dissipation of kinetic energy of the filtered velocity field by viscous stress; π [J/s], Sub-filter scale dissipation of kinetic energy; u [m/s], Velocity; D* [m], Characteristic diameter of the fire

Code availability Not applicable.

Data availability The simulation data is available upon request.

Declarations

Conflicts of interest The authors declare that they have no known competing financial interests or personal relationships that could have appeared to influence the work reported in this paper.

References

- Babrauskas V (2003) Ignition Handbook. Fire Science Publishers, Issaquah
- Berman M (1986) Hydrogen Behavior Nuclear Safety, CRC Recent Developments in Hydrogen Technology, Volume II, Chapter 2, p 35
- Abohamzeh E, Salehi F, Sheikholeslami M, Abbassi R, Khan F (2021) Review of hydrogen safety during storage transmission and applications processes. *J Loss Prev Process Ind* 72104569. <https://doi.org/10.1016/j.jlp.2021.104569>
- Finney MA, McAllister SS (2011) A Review of Fire Interactions and Mass Fires, Hindawi Publishing Corporation, Journal of Combustion, Volume 2011, Article ID 548328
- Gannouni S, Maad RB (2017) CFD analysis of smoke backlayering dispersion in tunnel fires with longitudinal ventilation. *Fire Mater* 41(6):598–613
- Gu X, Zhang J, Pan Y, Ni Y, Congming MA, Zhou W, Wang Y (2020) Hazard analysis on tunnel hydrogen jet fire based on CFD simulation of temperature field and concentration field. *Safety Sci* 122: 104532
- Hao D, Wang X, Zhang Y, Wang R, Chen G, Li J (2020) Experimental Study on Hydrogen Leakage and Emission of Fuel Cell Vehicles in Confined Spaces, *Automotive Innovation*, p 111–122
- He K, Cheng X, Yao Y, Shi L, Yang H, Cong W (2019) Characteristics of multiple pool fires in a tunnel with natural ventilation. *J Hazardous Mater* 369:261–267
- He K, Cheng X, Li YZ, Ingason H, Shi Z, Yang H, Zhang H (2021) Experimental study on flame characteristics of double fires in a naturally ventilated tunnel: Flame merging, flame tilt angle and flame height, *Tunnell Underground Space Technol* 114
- Hord J (1976) Is Hydrogen Safe? National Bureau of Standards (NBS) Technical Note 690
- L.H. Hu, L.F.Chen, L.Wu, Y.F.Li, J.Y.Zhang, N.Meng, An experimental investigation and correlation on buoyant gas temperature below ceiling in a slopping tunnel fire, *Appl Thermal Eng*, volume 51, Issues 1–2, 2013, Pg. 246–254
- Y. Huang, Y. Li, B. Dong, J. Li, Q. Liang, Numerical investigation on the maximum ceiling temperature and longitudinal decay in a sealing tunnel fire, *Tunn Undergr Space Technol*, 72, 2018, Pg. 120–130
- Y. Huo, Y. Gao, W.K. Chow, A study on ceiling jet characteristics in an inclined tunnel, *Tunn Undergr Space Technol* 50, 2015, Pg. 32–46
- C.C. Hwang, J.C. Edwards, The critical ventilation velocity in tunnel fires—a computer simulation, *Fire Saf J*, 40 (3), 2005, Pg. 213–244
- A. Król, M. Król, P. Koper, Numerical modeling of air velocity distribution in a road tunnel with a longitudinal ventilation system, *Tunn Undergr Space Technol*, 91, 2019, Pg. 103003
- B. Lewis and G. von Elbe, Combustion, flames and explosions of gases, 3rd ed., Academic Press, Orlando, 1987, pg. 717
- Ying Zhen Li, Study of fire and explosion hazards of alternative fuel vehicles in tunnels, *Fire Safety J*, Volume 110, December 2019, 102871
- Liu N, Liu Q, Lozano JS, Zhang L, Deng Z, Yao B, Zhu J, Satoh K (2013) Multiple fire interactions: a further investigation by burning rate data of square fire arrays. *Proc Combust Inst* 34:2555–2564
- Manoharan Y, Hosseini SE, Butler B, Alzahrani H, Senior BTF, Ashuri T, Krohn J (2019) Hydrogen fuel cell vehicles; current status and future Prospect. *Appl Sci* 9(11):2296
- McCarty RD, Hord J, Roder HM (1981) NBS Monograph 168, Selected Properties of Hydrogen (Engineering Design Data), Center for Chemical Engineering, National Engineering Laboratory, National Bureau of Standards, Boulder, CO 80303, published by U.S. Department of Commerce. U.S. Government Printing Office, Washington, D.C.
- McGrattan K, et al (2017) Fire Dynamics Simulator User's Guide (Sixth Edition), NIST Special Publication 1019
- NREL U.S. (2009) Department of Energy, Office of Energy Efficiency and Renewable Energy operated by the Alliance for sustainable energy, LLC, A Comparison of Hydrogen and Propane Fuels
- Palacios A, Rengel B (2020) Computational analysis of vertical and horizontal jet fires, *J Loss Prevent Process Indust* 65
- Rigas F, Sklavounos S (2005) Evaluation of hazards associated with hydrogen storage facilities. *Int J Hydrogen Energy* 30(13–14): 1501–1510
- Salehi F, Talei M, Hawkes ER, Yoo CS, Lucchini T, D'Errico G, Kook S (2015) A Comparative Study of Conditional Moment Closure Modelling for Ignition of iso-octane and n-heptane in Thermally Stratified Mixtures. *Flow Turbul Combustion* 95:1–28
- Staffell I, Scamman D, Abad AV, Balcombe P, Dodds PE, Ekins P, Shahd N, Warda KR (2019) The role of hydrogen and fuel cells in the global energy system. *Energy Environ Sci*, 463–491
- The Future of Hydrogen (2019) Seizing today's opportunities, Report prepared by IEA for the G20, Japan
- Xiaoyun Wang, Charles Fleischmann, Michael Spearpoint, Assessing the influence of fuel geometrical shape on fire dynamics simulator (FDS) predictions for a large-scale heavy goods vehicle tunnel fire experiment, *Case Stud Fire Safety* 5, 2016, Pg. 34–41
- Wang Q, Wang S, Liu H, Shen J, Shang F, Shi C, Tang F (2020) Characterization of ceiling smoke temperature profile and maximum temperature rise induced by double fires in a natural ventilation tunnel. *Tunnell Underground Space Technol* 96
- Wu Y (2008) Assessment of the impact of jet flame hazard from hydrogen cars in road tunnels. *Transport Res Part C: Emerg Technol* 16(2):246–254
- Zhang Y, Xing S, Chen R, Chen L, Li T, Mao P (2020) Experimental study on maximum temperature beneath tunnel ceiling under the condition of double fire sources. *Tunnell Underground Space Technol* 106
- Ming Zhao, Aiwu Fan, Buoyancy effects on hydrogen diffusion flames confined in a small tube, *Int J Hydrog Energy*, Volume 45, Issue 38, 2020, Pg. 19926–19919